

Minimizing the Profligacy of Searches with Reset

John C. Sunil, Richard A. Blythe, and Martin R. Evans
*SUPA, School of Physics and Astronomy, University of Edinburgh,
Peter Guthrie Tait Road, Edinburgh EH9 3FD, UK*

Satya N. Majumdar
Université Paris-Saclay, CNRS, LPTMS, 91405, Orsay, France
(Dated: April 10, 2024)

We introduce the profligacy of a search process as a competition between its expected cost and the probability of finding the target. The arbiter of the competition is a parameter λ that represents how much a searcher invests into increasing the chance of success. Minimizing the profligacy with respect to the search strategy specifies the optimal search. We show that in the case of diffusion with stochastic resetting, the amount of resetting in the optimal strategy has a highly nontrivial dependence on model parameters resulting in classical continuous transitions, discontinuous transitions and tricritical points as well as non-standard discontinuous transitions exhibiting re-entrant behavior and overhangs.

Searching is a task that arises in numerous domains. In nature, examples range from proteins locating their binding sites within the cell [1] to foraging by macro-organisms [2, 3]. In computer science, search algorithms have long been of fundamental interest [4] and have gained cultural importance in determining how the large and unstructured body of data that constitutes the internet is experienced by users [5]. Crossovers between these domains also exist, such as biologically-inspired optimization algorithms which can be applied to solve many and varied science and engineering problems [6]. A large literature has established optimal random search strategies, in the sense of optimizing the efficacy of the search [7–11].

In this work, we study a feature that is common to all such search processes, namely that increasing efficacy typically comes with a cost, for example, the amount of time or energy that must be invested or the complexity of the algorithm. A natural question is whether one can identify a point of diminishing return, i.e., a point beyond which investing more effort into the search is not compensated by sufficiently increased success. We answer this question by introducing a quantity called *profligacy* that expresses the cost-efficacy trade-off in a manner similar to Helmholtz free energy, wherein the search cost plays the role of energy, the success probability provides an analog to entropy, and a temperature-like quantity λ has the units of cost and characterizes how much effort a searcher is prepared to invest. We will show below that in the context of even fairly simple diffusive searches [12–14], the optimal strategy that arises from minimizing profligacy exhibits a rich phase diagram (presented in Fig. 2 below). By this we mean that one finds both continuous and discontinuous transitions between regimes in which the optimal search strategy switches. Moreover, the phase structure goes beyond what is normally seen at equilibrium, exhibiting re-entrant behavior and overhangs, to be detailed below.

We begin by deriving the profligacy ξ . Its origin is most clearly understood by appealing to an ensemble of K independent searchers, all of whom are following a strategy that is controlled by a parameter r . Associated with each searcher is a non-negative cost C that depends on the path that they have followed up to the allotted search time, t_f . Meanwhile, the overall efficacy of the search can be quantified in terms of the fraction of searchers that have located the target before t_f . As $K \rightarrow \infty$ this fraction converges to $P_s(r)$, the success probability for a single searcher (averaged over all possible search histories). Similarly, the total cost (across the ensemble) behaves asymptotically as $K\langle C(r) \rangle$, where $\langle C(r) \rangle$ is the mean cost for a single searcher (again averaged over all possible search histories). To implement the trade-off, we introduce a weighted efficacy $P_s(r)\omega(r)$ where the multiplicative factor $\omega(r)$ decreases with the total cost of the search. A natural choice is the exponential function $\omega(r) = \exp(-\langle C(r) \rangle/\lambda)$, since this lies in $[0, 1]$ for $\lambda \geq 0$, and we can identify the single parameter λ , which we call the investment, as a characteristic cost that each searcher is willing to invest. The point of diminishing return can now be defined as the value of r that maximizes the cost-weighted efficacy, or equivalently, that minimizes the profligacy

$$\xi = \langle C(r) \rangle - \lambda \ln P_s(r). \quad (1)$$

It is here that we recognize the structure of a Helmholtz free energy that was described above, and within which the variational parameter r relates to the search strategy.

We devote the rest of this work to determining how the search strategy that minimizes the profligacy changes as we vary the investment λ , within the framework of diffusive searches under stochastic resetting. In this context the searcher is modeled as a diffusive particle starting from the origin, which is reset instantaneously to the origin with rate r [12]. The search is successful if the searcher reaches a target located at distance m from the

origin. Early studies of such processes [12–15] demonstrated how resetting can allow the target to be found more quickly than through diffusion alone, replacing an infinite mean time to locate the target with some finite value. Moreover, there exists an optimal resetting rate r^* , which minimizes the mean time to find a target [12] and the value of r^* undergoes phase transitions as various control parameters are varied [16–29]. We emphasize that the optimization problem here is different, in that we seek to minimize the profligacy of a search constrained to end at a predetermined time t_f . Recently, the consequences of associating a cost with each reset, accounting for the consumption of time, fuel or some other finite resource, have been investigated [30–34] and the statistics of the cost as a function of r have been computed [33]. Here we consider a predetermined cost of the search, for example, where one purchases a search of duration t_f regardless of whether the target is found within that time. Thus the average cost $\langle C(r) \rangle$ does not depend on the target position (see SM [35] for further details). The resetting rate r furnishes a single key parameter, characterizing the search strategy, with which we may optimize the profligacy. We will focus on the transitions from a non-resetting optimal strategy, $r = 0$, to a non-zero optimal value of r .

We consider two classes of resetting models which differ in what happens at the end time t_f , as illustrated in Fig. 1. In the case of Resetting Brownian Motion (RBM) [12], the process is simply halted at t_f , meaning that searcher can be anywhere in space at time t_f . By contrast, a Resetting Brownian Bridge (RBB) [36] imposes the additional constraint that a searcher must return to the origin at time t_f . This models such situations as a rescue helicopter having to return to base to refuel after a prespecified flight time. The RBB ensemble is obtained from that of RBM by retaining only those trajectories that occupy the starting position at the completion time, t_f . In mechanical terms, this conditioning creates a time-dependent drift on the particle motion along with a resetting rate that diverges as t_f is approached, thereby guaranteeing a return to the origin [36].

Each reset i contributes a cost $c_i \geq 0$ which depends on the distance travelled to the origin in the reset. The number of resets N that occur up to the fixed time t_f is a random variable and fluctuates from trajectory to trajectory. The total cost, C , of a trajectory is obtained by summing over all N resets that occur along it:

$$C = \sum_{i=1}^N c_i = \sum_{i=1}^N c(|y_i|) \quad (2)$$

and the cost is zero if there is no reset in the trajectory. Here, $y_i = x_i/\sqrt{2Dt_f}$ is the rescaled (dimensionless) position just before the reset and the function $c(y)$ is the cost per reset. Similarly, it is convenient to use dimen-

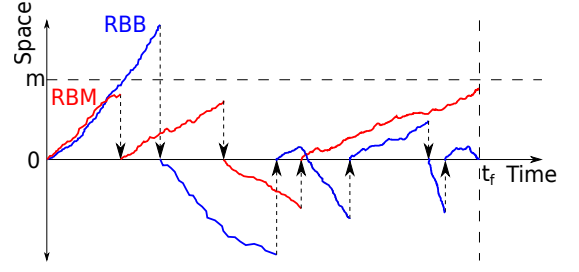


FIG. 1: Schematic trajectory for RBM (red) and RBB (blue). For RBM, the particle diffuses without constraint while for RBB the particle is constrained to return to the starting position at the completion time t_f . The vertical arrows represent resetting events. The searcher is considered to have found the target if it crosses $x = m$ in any of its excursions before t_f .

sionless, rescaled variables $R = rt_f$ and $M = m/\sqrt{2Dt_f}$, which eliminate the values of diffusion constant D and search time t_f from the discussion, and leave R , λ and M as the control variables. We will compare a linear, $c(y) = \sqrt{2}y$, and a quadratic, $c(y) = 2y^2$, cost per reset, since these are the simplest cases for practical applications, but, as we shall see, yield very different phase diagrams. The linear cost can be motivated as the time required to bring the particle back to the origin at a constant velocity [30, 31, 37]. Likewise, the quadratic cost can represent energy consumption, monetary cost or thermodynamic cost for the particle to reset [34, 38, 39].

Our aim now is to determine the optimal resetting strategy—that is, the value of $R = R^*$ that minimizes the profligacy (1)—for a given combination of target position M and investment λ . To achieve this, we must first evaluate the mean cost $\langle C \rangle$ and the probability of finding the target P_s . The resetting systems we consider have the appealing feature that these quantities can be calculated analytically, following recent progress in leveraging renewal properties of the process [33]. The success probability has been calculated for RBM in [12] and for RBB in [36]. The mean costs are derived in detail in the Supplemental Materials [35].

For the case of RBM, the explicit expressions are

$$\langle C \rangle_{\text{lin}}^{\text{RBM}} = \frac{e^{-R}}{\sqrt{\pi}} + \frac{(2R - 1) \operatorname{erf}(\sqrt{R})}{2\sqrt{R}} \quad (3)$$

$$\langle C \rangle_{\text{quad}}^{\text{RBM}} = \frac{2(R + e^{-R} - 1)}{R} \quad (4)$$

$$P_s^{\text{RBM}} = \int_{\Gamma} \frac{du}{2\pi i} e^u \frac{1}{u} \frac{R + u}{R + u e^{M\sqrt{2(u+R)}}} \quad (5)$$

where the subscripts lin and quad refer to the linear and quadratic cost functions, respectively. The success probability is expressed as an inverse Laplace transform, denoted by an integral over the Bromwich contour Γ . This form is sufficient to determine the phase diagrams nu-

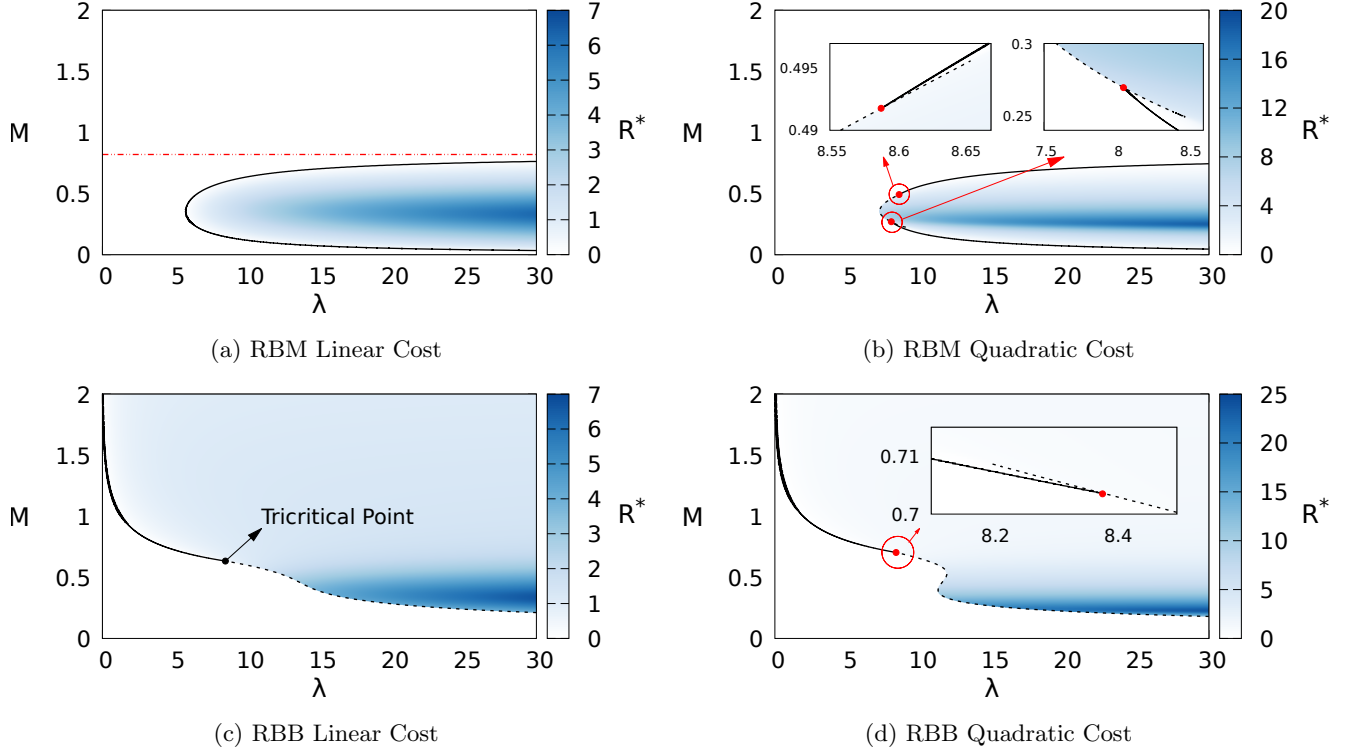


FIG. 2: Phase diagrams: heat map of R^* which minimizes profligacy (ξ) for 4 different cases: (a) RBM with linear cost (b) RBM with quadratic cost (c) RBB with linear cost and (d) RBB with quadratic cost. The phase boundaries delineate the boundary between regions of zero and non-zero R^* : a full line indicates a continuous transition and broken line a discontinuous transition. In (a) the horizontal red line indicates the threshold, M_T , above which there is no transition.

merically using a suitable inversion algorithm [40]. For RBB, meanwhile, we obtain

$$\langle C \rangle_{\text{lin}}^{\text{RBB}} = R\phi(R) \quad (6)$$

$$\langle C \rangle_{\text{quad}}^{\text{RBB}} = 2 - \frac{\text{erf}(\sqrt{R})}{\sqrt{R}}\phi(R) \quad (7)$$

$$P_s^{\text{RBB}} = \phi(R) \int_{\Gamma} \frac{du}{2\pi i} \frac{e^u \sqrt{u+R}}{u} \frac{R + ue^{-M\sqrt{2}\sqrt{u+R}}}{R + ue^{M\sqrt{2}\sqrt{u+R}}} \quad (8)$$

where $\phi(R) = \sqrt{\pi} [e^{-R} + \sqrt{\pi R} \text{erf} \sqrt{R}]^{-1}$.

In Fig. 2 we present the phase diagrams in the λ - M plane obtained by minimizing the profligacy with respect to R . We distinguish between the two different types of search (RBM and RBB) and the two different cost functions (linear and quadratic). In the unshaded regions, diffusing without resetting is optimal ($R^* = 0$), whereas in the shaded regions, a nonzero resetting rate yields the least profligate search. Along the solid lines, the optimal resetting rate R^* changes continuously across the phase boundary, whilst along the broken lines the optimal resetting rate jumps discontinuously. The nature of the transition is significant: a continuous transition implies

that a gradual introduction of resetting yields the optimal search strategy whereas a discontinuous transition implies a sudden switch of strategies to a finite resetting rate.

As we now discuss, the significant differences in the topology of the four phase diagrams derive from small qualitative distinctions in the behavior of $\langle C \rangle$ and P_s , i.e. Eqs. (3)–(8).

The easiest phase diagram to understand is that for RBM and a linear cost per reset (Fig. 2a) for which the cost (3) increases monotonically with the resetting rate (see SM Fig. S1). When the target is far from the origin (large M), the success probability (5) monotonically decreases (see SM Fig. S2). Thus for large M , $R^* = 0$ is always the optimal value. However for M below a threshold value M_T , the success probability initially increases with R and has a peak at some intermediate value of R . This implies that for sufficiently large λ the optimal resetting rate R^* is non zero. The transition to an optimal strategy that involves resetting can be understood by appealing to a Landau-like theory which implies a classical continuous phase transition into a resetting phase ($R^* > 0$) as λ is increased at fixed $M < M_T$.

We now turn to the case of a quadratic cost per reset,

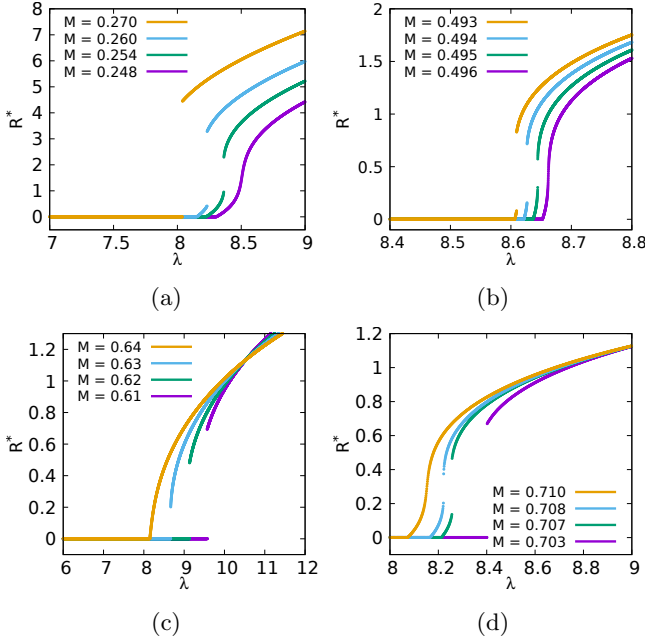


FIG. 3: Optimal resetting rate R^* versus λ for values of M in the regions where continuous and discontinuous transitions are in close proximity. Panels (a) and (b) RBM with quadratic cost: there are two different ranges of M (see Fig. 2) where on increasing λ , there is first a continuous transition followed by a discontinuous transition. The discontinuous jump in R^* closes at a non-zero value of R^* as M is varied and thus is not a usual tricritical point. Panel (c) RBB with linear cost: we have a usual tricritical point where the jump in discontinuity closes at $R^* = 0$. Panel (d) RBB with quadratic cost: similar to RBM the jump closes at non-zero value of R^* .

for which the mean cost no longer grows without bound as $R \rightarrow \infty$ but approaches a plateau (see SM Fig. S1). The effect of this on the RBM phase diagram, Fig. 2b, is the addition of a discontinuous transition line at intermediate M . Although this meets the continuous transition line at two points, it does not end there (as at tricritical points) but *extends* beyond them, thus creating overhangs (see insets). So as λ is increased, for particular choices of M , we find an initial continuous transition to a nonzero optimal resetting rate R^* very closely followed by a discontinuous jump in R^* as shown in Figs. 3a and 3b. This sequence of transitions implies an initial gradual introduction of resetting into the optimal search strategy then a sudden jump to a stronger resetting strategy.

In contrast to RBM, the success probability for a RBB search is a peaked function of R for all target positions M (see SM Fig. S2). The effect of this is that resetting always becomes beneficial for high enough λ . With a linear cost per reset (Fig. 2c), the transition is continuous for high M and discontinuous at low M , the two lines meeting at a classical tricritical point (see Fig. 3c) [29].

Finally, for the case of RBB with quadratic cost per reset (Fig. 2d), the shape of the phase boundary has developed a kink in comparison to the linear cost case. Similar to the case of RBM, the mean cost plateaus as $R \rightarrow \infty$, creating an overhang instead of a tricritical point. This overhang effect is evident in Fig. 3d, where we see both a continuous transition from $R^* = 0$ to $R^* > 0$ and a discontinuous jump between two nonzero values of R^* at a higher value of λ . As M is increased, the jump in the discontinuous transition goes to zero and we are left with a single continuous transition. If we consider fixing λ and increasing M , then in the region of the kink we have re-entrant behaviour into the $R^* = 0$ phase via a discontinuous transition.

To gain deeper insight into the nature of these transitions, we make a Landau-like expansion of the profligacy (1) in powers of R , valid for small values of R ,

$$\xi = a_0 + a_1 R + a_2 \frac{R^2}{2} + a_3 \frac{R^3}{6} + a_4 \frac{R^4}{24} + \dots, \quad (9)$$

with all the coefficients $a_i = a_i(\lambda, M)$. Due to the system not possessing an $R \rightarrow -R$ symmetry, we have to include all terms of the expansion. Related Landau-like expansions have been made in [24, 29]. The expansion of $\langle C \rangle$ is obtained directly from (3), (4) and (6), (7). We also require the expansion of P_s for the two resetting ensembles, which is obtained by expanding out the integrands of (5) and (8) in terms of R and integrating term by term. This procedure is carried out in detail in the SM [35].

The simplest case is when $a_2 > 0$ in the expansion (9) and we may ignore higher order terms. The curve of continuous transitions, $\lambda^*(M)$, is obtained by solving $a_1(\lambda, M) = 0$ for λ . This is the usual scenario for a continuous transition seen in equilibrium systems [41]. This simple scenario pertains in the case of RBM with a linear cost, where we saw in Fig. 2 that a continuous transition occurs on increasing λ , for sufficiently low M . The threshold value M_T is given by $\lambda^*(M_T) \rightarrow \infty$ and for $M > M_T$ no transition occurs. The exact value $M_T = 0.8198\dots$ that is obtained from this procedure provides the horizontal line in Fig. 2a.

The next case is where a_2 may be positive or negative according to parameters, but a_3 is positive. This is the case for RBB with linear cost, Fig. 2c. Then for $a_2 > 0$ we obtain a continuous transition at $a_1 = 0$ but for $a_2 < 0$ there is a discontinuous transition. A classical tricritical point occurs when $a_1 = a_2 = 0$ and $a_3 > 0$. To obtain the tricritical point, we set $a_2(\lambda^*, M) = 0$, which yields $(M^*, \lambda^*) = (0.6333, 8.4994)$ indicated by the filled circle in Fig. 2c.

The interesting non-classical overhangs that occur for both RBM and RBB with quadratic cost per reset (Figs. 2b and 2d) can be attributed to the coefficients satisfying $a_3 < 0$ and $a_4 > 0$. If we look for a tricritical point by solving $a_2(\lambda^*, M) = 0$ for M , we find at all such M^* that $a_3(\lambda^*, M^*) < 0$. This violates the condition

for a tricritical point, which is why overhangs emerge instead. Of course the predictions of a Landau-like theory for discontinuous transitions will only be quantitatively accurate for small R , nevertheless the correct qualitative behaviour is predicted.

In summary, we have introduced the profligacy ξ (1) as a tool to analyse the cost-efficacy trade-off in a search process. We have derived ξ from considering the efficacy, P_s , weighted by an exponential function of the cost expectation value $\langle C \rangle$. The simple framework of diffusion under stochastic resetting with rate r has allowed us to derive analytical expressions for P_s and $\langle C \rangle$ and thus to carry out the minimization of ξ . This has resulted in surprisingly rich phase diagrams, exhibiting classical continuous and discontinuous transitions, but also non-standard transitions with re-entrant behaviour and overhangs. These transitions imply changes of the optimal search strategy that may be gradual or sudden. We have shown that these transitions may be understood within a simple Landau-like expansion of the profligacy. As the profligacy just requires a cost and a measure of success as inputs, it has the potential for application in wider contexts. It would be of interest to see if the different classes of transition that we have identified here, arise more generally.

Acknowledgments—For the purpose of open access, the authors have applied a Creative Commons Attribution (CC BY) licence to any Author Accepted Manuscript version arising from this submission. JCS thanks the University of Edinburgh for the award of an EDC Scholarship.

-
- [1] P. Bressloff and J. M. Newby, [Stochastic models of intracellular transport](#), Rev. Mod. Phys. **85**, 135 (2013).
 - [2] G. M. Viswanathan, M. G. Da Luz, E. P. Raposo, and H. E. Stanley, *"The physics of foraging: an introduction to random searches and biological encounters."* (Cambridge University Press, 2011).
 - [3] W. J. Bell, *"Searching behaviour: the behavioural ecology of finding resources."* (Springer Science & Business Media, 2012).
 - [4] D. E. Knuth, *The art of computer programming v3: Sorting and searching* (Addison-Wesley, 1998).
 - [5] M. Henzinger, [Search technologies for the internet](#), Science **317**, 468 (2007).
 - [6] A. Darwish, [Bio-inspired computing: Algorithms review, deep analysis, and the scope of applications](#), Future Computing and Informatics Journal **3**, 231 (2018).
 - [7] G. M. Viswanathan, S. V. Buldyrev, S. Havlin, M. G. da Luz, E. P. Raposo, and H. E. Stanley, [Optimizing the success of random searches](#), Nature **401**, 911 (1999).
 - [8] O. Bénichou, M. Coppey, M. Moreau, P. Suet, and R. Voituriez, [Optimal search strategies for hidden targets](#), Phys. Rev. Lett. **94**, 198101 (2005).
 - [9] F. Bartumeus and J. Catalan, [Optimal search behavior and classic foraging theory](#), J. Phys. A **42**, 434002 (2009).
 - [10] O. Bénichou, C. Loverdo, M. Moreau, and R. Voituriez, [Intermittent search strategies](#), Rev. Mod. Phys. **83**, 81 (2011).
 - [11] E. A. Fronhofer, T. Hovestadt, and H.-J. Poethke, [From random walks to informed movement](#), Oikos **122**, 857 (2013).
 - [12] M. R. Evans and S. N. Majumdar, [Diffusion with stochastic resetting](#), Phys. Rev. Lett. **106**, 160601 (2011).
 - [13] M. R. Evans and S. N. Majumdar, [Diffusion with optimal resetting](#), J. Phys. A **44**, 435001 (2011).
 - [14] M. R. Evans, S. N. Majumdar, and G. Schehr, [Stochastic resetting and applications](#), J. Phys. A **53**, 193001 (2020).
 - [15] M. R. Evans, S. N. Majumdar, and K. Mallick, [Optimal diffusive search: nonequilibrium resetting versus equilibrium dynamics](#), J. Phys. A **46**, 185001 (2013).
 - [16] L. Kuśmierz, S. N. Majumdar, S. Sabhapandit, and G. Schehr, [First Order Transition for the Optimal Search Time of Lévy Flights with Resetting](#), Phys. Rev. Lett. **113**, 220602 (2014).
 - [17] D. Campos and V. Méndez, [Phase transitions in optimal search times: How random walkers should combine resetting and flight scales](#), Phys. Rev. E **92**, 062115 (2015).
 - [18] C. Christou and A. Schadschneider, [Diffusion with resetting in bounded domains](#), J. Phys. A **48**, 285003 (2015).
 - [19] S. Reuveni, [Optimal stochastic restart renders fluctuations in first passage times universal](#), Phys. Rev. Lett. **116**, 170601 (2016).
 - [20] U. Bhat, C. De Bacco, and S. Redner, [Stochastic search with Poisson and deterministic resetting](#), J. Stat. Mech. **2016**, 083401 (2016).
 - [21] A. Pal and S. Reuveni, [First passage under restart](#), Phys. Rev. Lett. **118**, 030603 (2017).
 - [22] A. Chechkin and I. M. Sokolov, [Random Search with Resetting: A Unified Renewal Approach](#), Phys. Rev. Lett. **121**, 050601 (2018).
 - [23] S. Ray, D. Mondal, and S. Reuveni, [Péclet number governs transition to acceleratory restart in drift-diffusion](#), J. Phys. A **52**, 255002 (2019).
 - [24] A. Pal and V. V. Prasad, [Landau-like expansion for phase transitions in stochastic resetting](#), Phys. Rev. Res. **1**, 032001 (2019).
 - [25] G. Mercado-Vásquez, D. Boyer, S. N. Majumdar, and G. Schehr, [Intermittent resetting potentials](#), J. Stat. Mech. **2020**, 113203 (2020).
 - [26] R. D. Schumm and P. C. Bressloff, [Search processes with stochastic resetting and partially absorbing targets](#), J. Phys. A **54**, 404004 (2021).
 - [27] G. Mercado-Vásquez, D. Boyer, and S. N. Majumdar, [Reducing mean first passage times with intermittent confining potentials: a realization of resetting processes](#), J. Stat. Mech. **2022**, 093202 (2022).
 - [28] M. Biroli, S. N. Majumdar, and G. Schehr, [Critical number of walkers for diffusive search processes with resetting](#), Phys. Rev. E **107**, 064141 (2023).
 - [29] D. Boyer, G. Mercado-Vásquez, S. N. Majumdar, and G. Schehr, [Optimizing the random search of a finite-lived target by a Lévy flight](#), Phys. Rev. E **109**, L022103 (2024).
 - [30] A. Pal, L. Kuśmierz, and S. Reuveni, [Search with home returns provides advantage under high uncertainty](#), Phys. Rev. Res. **2**, 043174 (2020).
 - [31] A. Bodrova and I. Sokolov, [Resetting processes with non-instantaneous return](#), Phys. Rev. E **101**, 052130 (2020).
 - [32] B. D. Bruyne and F. Mori, [Resetting in stochastic opti-](#)

- mal control., Phys. Rev. Res. **5**, 013122 (2023).
- [33] J. C. Sunil, R. A. Blythe, M. R. Evans, and S. N. Majumdar, [The cost of stochastic resetting.](#), J. Phys. A **56**, 395001 (2023).
 - [34] F. Mori, K. S. Olsen, and S. Krishnamurthy, [Entropy production of resetting processes](#), Phys. Rev. Res. **5**, 023103 (2023).
 - [35] See Supplemental Material at [URL will be inserted by publisher] for details of the calculations.
 - [36] B. De Bruyne, S. N. Majumdar, and G. Schehr, [Optimal Resetting Brownian Bridges via Enhanced Fluctuations.](#), Phys. Rev. Lett. **128**, 200603 (2022).
 - [37] A. Bodrova and I. Sokolov, [Brownian motion under non-instantaneous resetting in higher dimensions](#), Phys. Rev. E **102**, 032129 (2020).
 - [38] O. Tal-Friedman, A. Pal, A. Sekhon, S. Reuveni, and Y. Roichman, [Experimental realization of diffusion with stochastic resetting](#), J. Phys. Chem. Lett. **11**, 7350 (2020).
 - [39] B. Besga, A. Bovon, A. Petrosyan, S. N. Majumdar, and S. Ciliberto, [Optimal mean first-passage time for a Brownian searcher subjected to resetting: experimental and theoretical results](#), Phys. Rev. Res. **2**, 032029(R) (2020).
 - [40] J. Abate and W. Whitt, [A Unified Framework for Numerically Inverting Laplace Transforms](#), INFORMS Journal on Computing **18**, 408 (2006).
 - [41] N. Goldenfeld, [Lectures on phase transitions and the renormalization group](#) (CRC Press, 2018).
 - [42] S. Redner, [A Guide to First-Passage Processes](#) (Cambridge University Press, 2001).

Minimizing the Profligacy of Searches with Reset

Supplemental Material

John C. Sunil, Richard A. Blythe, and Martin R. Evans
*SUPA, School of Physics and Astronomy, University of Edinburgh,
 Peter Guthrie Tait Road, Edinburgh EH9 3FD, UK*

Satya N. Majumdar
Université Paris-Saclay, CNRS, LPTMS, 91405, Orsay, France
 (Dated: April 10, 2024)

This Supplemental Material details the calculations of the mean cost (Section I) and the success probability (Section II) in diffusion with resetting. Section III sets out the Landau-like expansion of the profligacy and the procedure for determining where phase boundaries lie. Finally, we briefly expand in Section IV on the interpretation of the profligacy function introduced in the main text as it applies to the case of predetermined search strategies.

I. DERIVATION OF THE MEAN COST

The key quantity that is required to determine the mean total cost incurred in a diffusive resetting process is $\Omega_r(C, t_f)$, the statistical weight of trajectories that start at the origin at $t = 0$, return to the origin as a Poisson process at rate r , end at a predetermined time $t = t_f$ and incur a total cost C . These statistical weights will differ in the ensemble where the endpoint of the trajectory is free (as in Resetting Brownian Motion, RBM) or constrained to lie at the origin (as in a Resetting Brownian Bridge, RBB). Once this quantity is known, we can determine the mean cost over such trajectories as

$$\langle C \rangle = \frac{\int dC C \Omega_r(C, t_f)}{\int dC \Omega_r(C, t_f)}. \quad (S1)$$

An explicit expression for $\Omega_r(C, t_f)$ is obtained from a renewal equation. The idea is to consider the evolution from the start of the process until either one of two things happens. The first possibility is that the particle resets for the first time at some time $0 \leq t \leq t_f$, after which the entire process restarts from the origin, with the remainder of the trajectory lasting a time $t - t_f$ and incurring a cost $C - c(x)$, where $c(x) \geq 0$ is the cost of resetting from the point x to the origin. In this case, the particle resets with probability $e^{-rt} r dt$ in the interval $[t, t + dt]$, and is distributed over space as $G(x; t)$ which is the Green function for diffusion,

$$G(x; t) = \frac{1}{\sqrt{4\pi Dt}} e^{-\frac{(x-x_0)^2}{4Dt}} \quad (S2)$$

where D is the diffusion constant. The second possibility is the particle reaches the point x at time t_f without resetting. This event arises with probability e^{-rt_f} , incurs zero cost and we allow only those endpoints x that fall within the set E . For the case of RBM, E is the entire real line, whereas for RBB, E is the origin.

Expressing these two possibilities as a renewal equation, we find

$$\Omega_r(C, t_f) = \int_0^{t_f} dt r e^{-rt} \int_{-\infty}^{\infty} dx G(x; t) \Omega_r(C - c(x), t_f - t) + e^{-rt_f} \delta(C) \int_E dx G(x; t_f). \quad (S3)$$

The first term is a convolution and thus the recursion can be solved by introducing the double Laplace transform

$$\tilde{\Omega}_r(p, s) = \int_0^{\infty} dC e^{-pC} \int_0^{\infty} dt_f e^{-st_f} \Omega_r(C, t_f). \quad (S4)$$

Note on notation Here we have used $\tilde{\Omega}_r(N, p|x_0, s)$ to indicate a double Laplace transform. We will also use a tilde symbol to denote single Laplace transforms of a single time variable, e.g. $\tilde{G}(x; s)$, below. The arguments of the function should make clear the number of Laplace variables. In certain places, for convenience, we will use $\mathcal{L}_{t \rightarrow s}$ to indicate Laplace transform to Laplace variable s and $\mathcal{L}_{s \rightarrow t}^{-1}$ to indicate Laplace inversion to the time domain.

Laplace transforming (S3) with respect to both arguments and rearranging, we find

$$\tilde{\Omega}_r(p, s) = \frac{\tilde{K}(r + s)}{1 - r \tilde{W}(p, r + s)} \quad (S5)$$

where

$$\tilde{K}(s) = \int_E dx \int_0^\infty dt_f e^{-st_f} G(x; t_f) = \int_E dx \tilde{G}(x; s) \quad (\text{S6})$$

$$\tilde{W}(p, s) = \int_{-\infty}^\infty dx e^{-pc(x)} \int_0^\infty dt e^{-st} G(x; t) = \int_{-\infty}^\infty dx e^{-pc(x)} \tilde{G}(x; s) \quad (\text{S7})$$

and we have from (S2) that

$$\tilde{G}(x, s) = \frac{1}{2\sqrt{Ds}} e^{-\sqrt{\frac{s}{D}}|x|}. \quad (\text{S8})$$

We see that the function $\tilde{K}(s)$ is determined by the constraint placed on the endpoint of the trajectory, and that $\tilde{W}(p, s)$ depends on the functional form of the cost. Once these functions have been determined for the cases of interest, we can obtain the mean cost as a function of t_f from (S1) via

$$\langle C \rangle = \frac{\mathcal{L}_{s \rightarrow t_f}^{-1} \{ -\partial_p \tilde{\Omega}_r(p, s) |_{p \rightarrow 0} \}}{\mathcal{L}_{s \rightarrow t_f}^{-1} \{ \tilde{\Omega}_r(p, s) |_{p \rightarrow 0} \}}. \quad (\text{S9})$$

Taking the limit $p \rightarrow 0$, we find that the functions to be inverted to obtain the numerator and denominator, respectively, are

$$-\partial_p \tilde{\Omega}_r(p, s) \Big|_{p \rightarrow 0} = \frac{r(r+s)^2}{s^2} \tilde{K}(r+s) \int_{-\infty}^\infty dx c(x) \tilde{G}(x; r+s) \quad (\text{S10})$$

$$\tilde{\Omega}_r(p, s) \Big|_{p \rightarrow 0} = \frac{r+s}{s} \tilde{K}(r+s). \quad (\text{S11})$$

A. Resetting Brownian Motion (RBM)

For the case of RBM, the trajectory endpoint is unconstrained, and the integral in (S6) is over all x . For any properly normalized distribution of endpoints we then have $\tilde{K}(s) = \frac{1}{s}$ and the denominator in (S9) is unity. It thus remains to compute the numerator by inverting (S10) for the cost function of interest. In the main text we consider power-law cost functions,

$$c(x) = 2^{n/2} |y|^n \quad \text{where} \quad y = \frac{x}{\sqrt{2Dt_f}}, \quad (\text{S12})$$

specifically the linear and quadratic cases, $n = 1$ and $n = 2$. Substituting into (S10) yields

$$\langle C \rangle_n^{\text{RBM}} = \frac{\Gamma(n+1)}{t_f^{n/2}} \mathcal{L}_{s \rightarrow t_f}^{-1} \left\{ \frac{r}{s^2} \frac{1}{(r+s)^{n/2}} \right\} = \frac{\Gamma(n+1)}{R^{n/2}} \frac{R\gamma(\frac{n}{2}, R) - \gamma(\frac{n}{2} + 1, R)}{\Gamma(\frac{n}{2})} \quad (\text{S13})$$

where $R = rt_f$ is the dimensionless resetting rate, and $\gamma(s, x)$ is the lower incomplete Gamma function,

$$\gamma(s, x) = \int_0^x du u^{s-1} e^{-u}. \quad (\text{S14})$$

Note that this result is obtained by recognising the Laplace transform in (S13) as the convolution of t with $\frac{1}{\Gamma(n/2)} t^{n/2-1} e^{-rt}$, evaluated at t_f . Note further that $\langle C \rangle_0^{\text{RBM}} = R$ and that for the special cases $n = 1$ ('lin') and $n = 2$ ('quad') considered in the main text, we have

$$\langle C \rangle_{\text{lin}}^{\text{RBM}} = \frac{e^{-R}}{\sqrt{\pi}} + \frac{(2R-1) \operatorname{erf}(\sqrt{R})}{2\sqrt{R}} \quad (\text{S15})$$

$$\langle C \rangle_{\text{quad}}^{\text{RBM}} = \frac{2(R + e^{-R} - 1)}{R}, \quad (\text{S16})$$

where we have used

$$\Gamma(\frac{1}{2}) = \sqrt{\pi}, \quad \gamma(\frac{1}{2}, x) = \sqrt{\pi} \operatorname{erf}(\sqrt{x}) \quad \text{and} \quad \gamma(1, x) = 1 - e^{-x} \quad (\text{S17})$$

along with the recursion relation

$$\gamma(s+1, x) = s\gamma(s, x) - x^s e^{-x}. \quad (\text{S18})$$

B. Resetting Brownian Bridge (RBB)

For the RBB, the calculation is a little more complex due to the constraint on the trajectory endpoint. Taking E to comprise just the point at the origin in (S6) we now have $\tilde{K}(s) = \frac{1}{2\sqrt{Ds}}$ and the denominator of (S9) takes the form

$$\mathcal{L}_{s \rightarrow t_f}^{-1} \{ \tilde{\Omega}_r(p, s) |_{p \rightarrow 0} \} = \frac{1}{2\sqrt{D}} \mathcal{L}_{s \rightarrow t_f}^{-1} \left\{ \left(1 + \frac{r}{s} \right) \frac{1}{\sqrt{r+s}} \right\} = \frac{e^{-rt_f} + \sqrt{\pi r t_f} \operatorname{erf}(\sqrt{r t_f})}{2\sqrt{\pi D t_f}}. \quad (\text{S19})$$

Again, the inversion can be performed by recognising as a convolution.

Turning now to the numerator, we find for $c(x)$ given by (S12) that

$$\mathcal{L}_{s \rightarrow t_f}^{-1} \{ -\partial_p \tilde{\Omega}_r(p, s) |_{p \rightarrow 0} \} = \frac{1}{2\sqrt{D}} \frac{\Gamma(n+1)}{t_f^{n/2}} \mathcal{L}_{s \rightarrow t_f}^{-1} \left\{ \frac{r}{s^2} \frac{1}{(r+s)^{(n-1)/2}} \right\}. \quad (\text{S20})$$

Comparing with (S13) we see that

$$\mathcal{L}_{s \rightarrow t_f}^{-1} \{ -\partial_p \tilde{\Omega}_r(p, s) |_{p \rightarrow 0} \} = \frac{n}{2\sqrt{D t_f}} \langle C \rangle_{n-1}^{\text{RBM}} \quad (\text{S21})$$

and by dividing by the denominator (S19) we find

$$\langle C \rangle_n^{\text{RBB}} = \frac{n\sqrt{\pi} \langle C \rangle_{n-1}^{\text{RBM}}}{e^{-R} + \sqrt{\pi R} \operatorname{erf}(\sqrt{R})}, \quad (\text{S22})$$

recalling that $R = r t_f$. For the special cases $n = 1$ and $n = 2$ we have

$$\langle C \rangle_{\text{lin}}^{\text{RBB}} = \frac{\sqrt{\pi} R}{e^{-R} + \sqrt{\pi R} \operatorname{erf}(\sqrt{R})} \quad (\text{S23})$$

$$\langle C \rangle_{\text{quad}}^{\text{RBB}} = 2 - \sqrt{\frac{\pi}{R}} \frac{\operatorname{erf}(\sqrt{R})}{e^{-R} + \sqrt{\pi R} \operatorname{erf}(\sqrt{R})}. \quad (\text{S24})$$

We compare the functional forms of the mean cost between the two ensembles in Fig. S1. Fig. S1a shows how the mean linear cost behaves with R , and is seen to increase indefinitely as $R \rightarrow \infty$ as \sqrt{R} . Corresponding plots for the mean quadratic cost are in Fig. S1b. Unlike the case for the linear cost, the mean total quadratic cost saturates as $R \rightarrow \infty$.

II. DERIVATION OF SUCCESS PROBABILITIES

A. Resetting Brownian Motion (RBM)

For a Resetting Brownian Motion, the probability of reaching a target at position m by time t_f can be obtained from the target's survival probability which was given as Eq. (6) in [12]. Noting that the target surviving corresponds to an unsuccessful search, we find that the success probability is given by the inverse Laplace transform

$$P_s^{\text{RBM}} = \int_{\Gamma} \frac{ds}{2\pi i} e^{s t_f} \frac{1}{s} \frac{r+s}{r + s e^{\sqrt{\frac{r+s}{D}} m}}. \quad (\text{S25})$$

where Γ is the Bromwich contour. By introducing rescaled variables $u = s t_f$, $R = r t_f$ and $M = \frac{m}{\sqrt{2 D t_f}}$, we obtain the form presented in the main text,

$$P_s^{\text{RBM}} = \int_{\Gamma} \frac{du}{2\pi i} e^u \frac{1}{u} \frac{R+u}{R+u e^{M\sqrt{2u+R}}}. \quad (\text{S26})$$

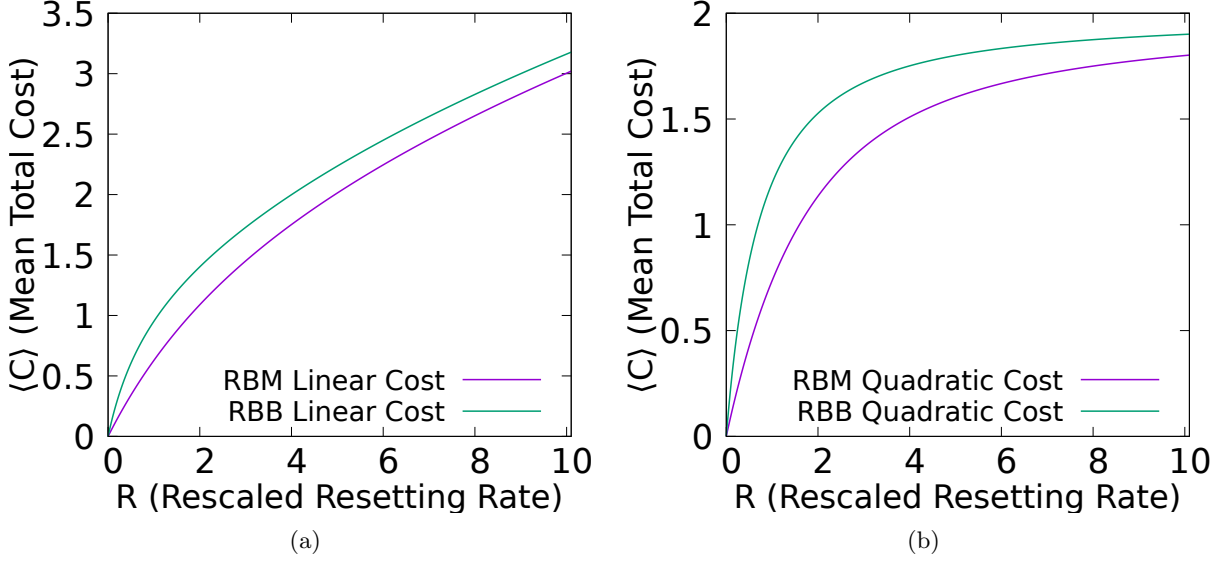


FIG. S1: Comparison of mean total cost $\langle C \rangle$ for (a) linear cost and (b) quadratic cost per reset for RBM and RBB. It can be seen that the costs increase monotonically for both the cases. This is consistent with the intuition that more frequent resets will incur a higher cost. Although in the case of a linear cost the mean cost increases indefinitely with R we find that in the case of a quadratic cost the mean cost saturates as $R \rightarrow \infty$.

B. Resetting Brownian Bridge (RBB)

The success probability for a Resetting Brownian Bridge is provided as Eq. (54) in the Supplemental Material of Ref. [36]. In the notation of the present work, this reads

$$P_s^{\text{RBB}} = \phi(R) \int_{\Gamma} \frac{du}{2\pi i} e^u \frac{\sqrt{u+R}}{u} \frac{R + ue^{-M\sqrt{2}\sqrt{u+R}}}{R + ue^{M\sqrt{2}\sqrt{u+R}}} \quad \text{where} \quad \phi(R) = \frac{\sqrt{\pi}}{e^{-R} + \sqrt{\pi R} \text{erf}(\sqrt{R})}. \quad (\text{S27})$$

We can plot the success probabilities (S26) and (S27) by performing the inverse Laplace transforms numerically [40]. In Figure S2a, we plot the two functions obtained at fixed $M = 1$. For RBM, we find that the success probability decreases monotonically with R , whilst for RBB, the function is peaked at some nonzero resetting rate R . When M is reduced to $\frac{1}{2}$, Figure S2b, we find that both functions are peaked.

III. LANDAU-LIKE EXPANSION FOR PROFLIGACY (ξ)

To gain deeper insight into the nature of the transitions observed in the main text, we make a Landau-like expansion of the profligacy (1)

$$\xi = \langle C \rangle - \lambda \ln P_s \quad (\text{S28})$$

in powers of R , valid for small values of R , which we define as

$$\xi = a_0 + a_1 R + a_2 \frac{R^2}{2} + a_3 \frac{R^3}{6} + a_4 \frac{R^4}{24} + \dots, \quad (\text{S29})$$

where $a_i = a_i(\lambda, M)$. Due to the system not possessing an $R \rightarrow -R$ symmetry, we have to include all terms of the expansion. The expansion of $\langle C \rangle$ can be obtained from performing a Taylor expansions of the mean total costs given by (S15), (S16), (S23) or (S24), as appropriate for the case of interest.

We also need to expand P_s in each ensemble, expressions for which are given by the integrals (S26) and (S27). To

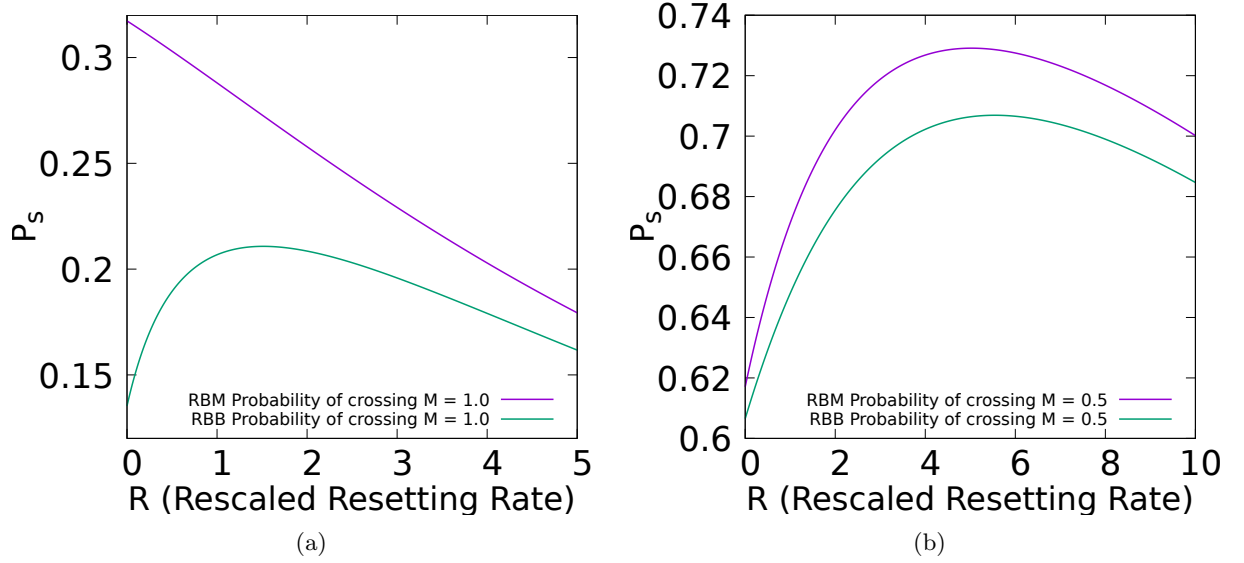


FIG. S2: Comparison of probability of finding the target (P_s) as a function R for (a) $M = 1.0$ and (b) $M = 0.5$. For RBM (purple), P_s can initially be a decreasing of increasing function depending on the value of M , whereas for RBB (green) P_s always increases initially with resetting, reaches a maximum then decreases for large R .

perform these expansions, it is helpful to define $s = u + R$, so that they become

$$P_s^{\text{RBM}} = e^{-R} \int_{\Gamma} \frac{du}{2\pi i} e^u \frac{1}{s - R} \frac{s}{R + (s - R)e^{M\sqrt{2}s}}, \quad (\text{S30})$$

$$P_s^{\text{RBB}} = \frac{\sqrt{\pi}e^{-R}}{\sqrt{\pi R} \operatorname{erf}(\sqrt{R}) + e^{-R}} \int_{\Gamma} \frac{ds}{2\pi i} e^s \frac{\sqrt{s}}{s - R} \frac{R + (s - R)e^{-M\sqrt{2}s}}{R + (s - R)e^{M\sqrt{2}s}}. \quad (\text{S31})$$

The procedure now is to expand these expressions as a power series in R , and invert term-by-term. Up to second order, we find for the RBM case the expansion

$$P_s^{\text{RBM}} = g_0(M) + g_1(M)R + g_2(M)\frac{R^2}{2} + \dots, \quad (\text{S32})$$

where the coefficients $g_i(M)$ are given by the integrals

$$g_0(M) = \int_{\Gamma} \frac{ds}{2\pi i} e^s \frac{e^{-\sqrt{2}M\sqrt{s}}}{s} = \operatorname{erfc}\left(\frac{M}{\sqrt{2}}\right) \quad (\text{S33})$$

$$g_1(M) = \int_{\Gamma} \frac{ds}{2\pi i} e^s \frac{e^{-2\sqrt{2}M\sqrt{s}} \left(-1 - e^{\sqrt{2}M\sqrt{s}}(-2 + s)\right)}{s^2} \quad (\text{S34})$$

$$g_2(M) = \int_{\Gamma} \frac{ds}{2\pi i} e^s \frac{e^{-3\sqrt{2}M\sqrt{s}} \left(2 + 2e^{\sqrt{2}M\sqrt{s}}(-3 + s) + e^{2\sqrt{2}M\sqrt{s}}(6 - 4s + s^2)\right)}{s^3}, \quad (\text{S35})$$

each of which can, like $g_0(M)$, be expressed in a closed form in terms of error functions. Explicit expressions are provided in an accompanying Mathematica notebook uploaded to [DataShare](#).

Similarly for RBB, we have

$$P_s^{\text{RBB}} = h_0(M) + h_1(M)R + h_2(M)\frac{R^2}{2} + \dots, \quad (\text{S36})$$

where

$$h_0(M) = \int_{\Gamma} \frac{ds}{2\pi i} e^s \frac{e^{-2\sqrt{2}M\sqrt{s}} \sqrt{\pi}}{\sqrt{s}} = e^{-2M^2}, \quad (\text{S37})$$

$$h_1(M) = \int_{\Gamma} \frac{ds}{2\pi i} e^s \frac{e^{-3\sqrt{2}M\sqrt{s}} \sqrt{\pi} \left(-1 + e^{2\sqrt{2}M\sqrt{s}} + e^{\sqrt{2}M\sqrt{s}}(1-2s) \right)}{s^{3/2}}, \quad (\text{S38})$$

$$h_2(M) = \int_{\Gamma} \frac{ds}{2\pi i} e^s \frac{2e^{-4\sqrt{2}M\sqrt{s}} \sqrt{\pi} \left(3 + 6e^{\sqrt{2}M\sqrt{s}}(-1+s) - 6e^{3\sqrt{2}M\sqrt{s}}(-1+s) + 2e^{2\sqrt{2}M\sqrt{s}}s(-3+4s) \right)}{3s^{5/2}} \quad (\text{S39})$$

and which again have closed-form expressions.

A similar process can be used to obtain the terms beyond the quadratic term. Note that in $R \rightarrow 0$ limit, (S32) and (S36) reduce to known results without resetting: $P_s^{\text{RBM}} = \text{erfc}\left(\frac{M}{\sqrt{2}}\right)$ [42] and $P_s^{\text{RBB}} = e^{-2M^2}$ [36].

The coefficients a_i in (S29) can be written in terms of the terms of expansion of P_S as

$$a_0 = C_0 - \lambda \log(g_0), \quad (\text{S40})$$

$$a_1 = C_1 - \lambda \frac{g_1}{g_0}, \quad (\text{S41})$$

$$a_2 = \frac{C_2}{2} - \lambda \frac{(-g_1^2 + g_0 g_2)}{2g_0^2}, \quad (\text{S42})$$

$$a_3 = \frac{C_3}{6} - \lambda \frac{(2g_1^3 - 3g_0 g_1 g_2 + g_0^2 g_3)}{6g_0^3}, \quad (\text{S43})$$

$$a_4 = \frac{C_4}{24} - \lambda \frac{(-6g_1^4 + 12g_0 g_1^2 g_2 - 3g_0^2 g_2^2 - 4g_0^2 g_1 g_3 + g_0^3 g_4)}{24g_0^4}, \quad (\text{S44})$$

where $C_n = \left. \frac{d^n \langle C \rangle}{dR^n} \right|_{R \rightarrow 0^+}$. The g_i should be substituted with h_i in the RBB case.

We now discuss the different cases that occur for transitions in the global minimum of the profligacy ξ as we vary λ .

A. Classical continuous transition

In this case $a_2 > 0$ in the expansion (S29) and may ignore higher order terms. The curve of continuous transition occurs when $a_1 = 0$. This is the usual scenario for a continuous transition seen in equilibrium systems [41]. Continuous transition lines are seen in all four panels of Fig. 2.

For the case of RBM the continuous transition condition, $a_1(\lambda, M) = 0$, is satisfied at $\lambda^*(M)$ given by

$$\lambda^* = \left. \frac{d \langle C \rangle^{\text{RBM}}}{dR} \right|_{R \rightarrow 0^+} \times \frac{\text{erfc}\left(\frac{M}{\sqrt{2}}\right)}{g_1(M)}, \quad (\text{S45})$$

with $\left. \frac{d \langle C \rangle_{\text{lin}}^{\text{RBM}}}{dR} \right|_{R \rightarrow 0^+} = \frac{4}{3\sqrt{\pi}}$ and $\left. \frac{d \langle C \rangle_{\text{quad}}^{\text{RBM}}}{dR} \right|_{R \rightarrow 0^+} = 1$. However, since we consider the investment λ , to act as a penalty if the searcher does not find the target, we require $\lambda > 0$. But $g_1(M) < 0$ for $M > 0.8198$ which suggests that a continuous transition cannot exist for RBM if the rescaled distance to the target is greater than $M = 0.8198$. Further, $a_1(\lambda^*, M) > 0$ for all values $M < 0.8198$, which implies that the system has a continuous transition for all values of $M < 0.8198$. This exactly matches with the result obtained in the FIG. 2a and 2b where no transitions are observed beyond the critical value of M .

For the case of RBB, the continuous transition condition, $a_1(\lambda, M) = 0$, is satisfied at $\lambda^*(M)$. There we obtain the curve of continuous transition ($a_1(\lambda, M) = 0$) to be

$$\lambda^* = \left. \frac{d \langle C \rangle}{dR} \right|_{R \rightarrow 0^+} \times \frac{e^{-2M^2}}{h_1(M)}. \quad (\text{S46})$$

where we have the derivatives $\left. \frac{d \langle C \rangle_{\text{lin}}^{\text{RBB}}}{dR} \right|_{R \rightarrow 0^+} = \sqrt{\pi}$ and $\left. \frac{d \langle C \rangle_{\text{quad}}^{\text{RBB}}}{dR} \right|_{R \rightarrow 0^+} = \frac{8}{3}$. Since $h_1(M) > 0$ for all values of M , we obtain a solution for $a_1 = 0$ for all values of M for RBB. For small values of λ^* this corresponds to a continuous

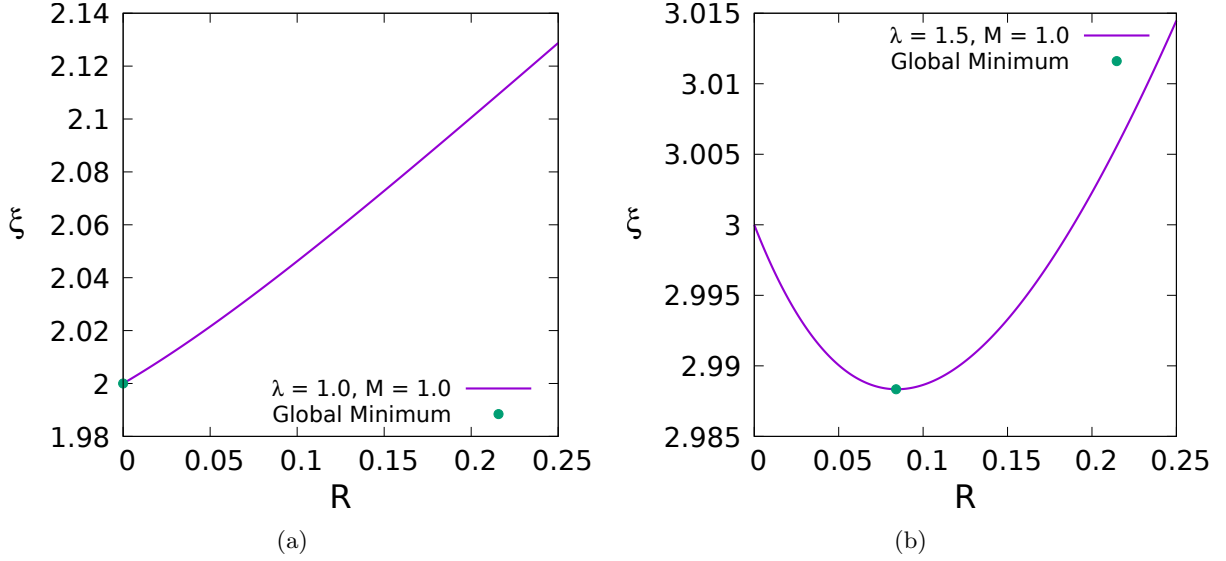


FIG. S3: The figure presents classical continuous transition observed in ξ for the case of RBB with linear cost per reset when λ is varied for $M = 1.0$. (a) The global minimum which is at $R^* = 0$ initially continuously transitions to the new global minimum R^* in (b) as λ is varied.

transition, however for large values of λ^* we find that $a_2 < 0$ and we have to consider classical discontinuous transition which we now discuss.

B. Classical discontinuous transition

A discontinuous transition may occur when a_1 is positive, a_2 is negative but a_3 is positive. Then we have a local minimum in the profligacy at a non-zero value of R in addition to a boundary minimum at $R = 0$. If on increasing λ the global minimum switches between these two local minima, we have a jump in R^* from a zero to a non-zero value. This is the classical scenario for a discontinuous transition. A classical tricritical point occurs when a continuous transition line meets a discontinuous transition line, which occurs when $a_1 = a_2 = 0$.

A classical tricritical point occurs in the case of RBB with linear cost as is seen in Fig. 2c. Then for $a_2 > 0$ we obtain a continuous transition at $a_1 = 0$ but for $a_2 < 0$ there is a discontinuous transition and if $a_1 = a_2 = 0$ (and $a_3 > 0$), we obtain a tricritical point. To obtain the tricritical point for RBB with linear cost per reset, we set $a_2(\lambda^*, M) = 0$, which gives

$$e^{-2M^*} \frac{d^2 \langle C \rangle}{dR^2} \Big|_{R \rightarrow 0^+} + e^{2M^*} \lambda^* h_1^2(M^*) - \lambda^* h_2(M^*) = 0, \quad (\text{S47})$$

which upon solving yields the tricritical point $(M^*, \lambda^*) = (0.6333, 8.4994)$. For λ approaching this point from above we have a classical discontinuous transition

C. Non-classical discontinuous transition

Finally we address an interesting scenario, which to our knowledge is a non-standard way of generating discontinuous transitions. This occurs when $a_3 < 0$ and $a_4 > 0$ and we retain terms up to R^4 in the Landau-like expansion. This is the case for both RBM and RBB with quadratic cost per reset in an intermediate range of M . The quartic expansion in R allows two local minima in the profligacy if $a_1 < 0$, or one local minimum, plus a boundary minimum at $R = 0$, if $a_1 > 0$. In the latter case either a discontinuous transition to a non-zero value of R^* can occur when the local minimum becomes the global minimum, or a continuous transition can occur when a_1 becomes negative; in the former case a discontinuous transition between two non-zero values of R^* can occur when the global minimum switches between the two local minima. A sequence of a continuous transition (when a_1 turns negative) followed by a discontinuous transition (when the global minimum switches between the subsequent two local minima) generates the overhangs

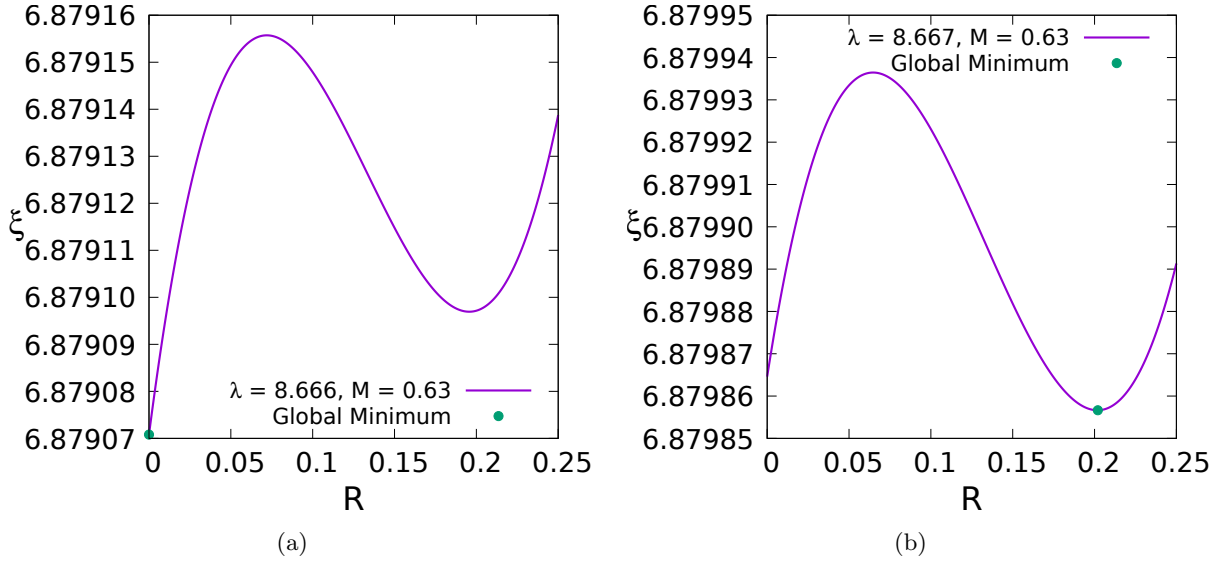


FIG. S4: The figure presents classical discontinuous transition observed in ξ for the case of RBB with linear cost per reset when λ is varied for $M = 0.63$. (a) The global minimum which is at $R^* = 0$ initially discontinuously transitions to the new global minimum R^* in (b) when the local minima becomes the new global minima as λ is varied.

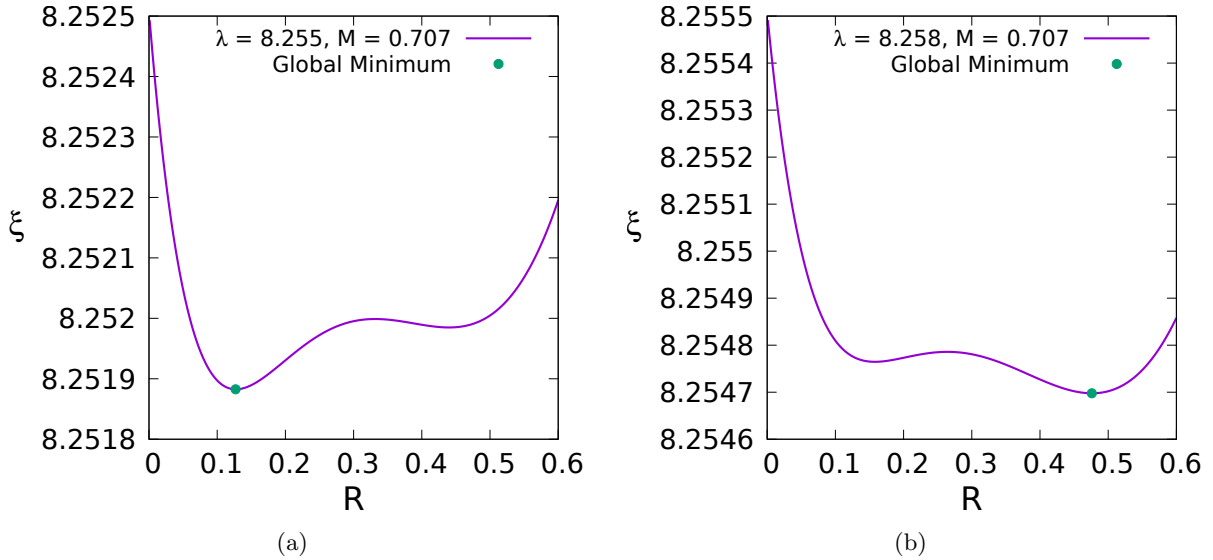


FIG. S5: The figure presents the non-classical discontinuous transition occurs observed in RBB with quadratic cost per reset as λ is varied for $M = 0.707$. (a) The global minimum initially emerges continuously from $R = 0$ as λ is varied. (b) As λ is further increased, the second minimum becomes the global minima and there is a discontinuous transition of the optimal value R^* to the new global minimum.

seen in Figs. 2b,2d. Thus the red dots in Figs. 2b,2d are not classical tricritical points as can be verified by evaluating $a_2(\lambda^*, m) = 0$. For RBM evaluating this results in two different values $m_{1,2}^*$, but evaluating the coefficient of R^3 gives $a_3(\lambda^*, m_{1,2}^*) < 0$.

Finally we comment that, generally speaking, if the coefficients of R^2 or higher turn out to be negative, it indicates that a discontinuous transition might be possible. But the prediction of discontinuous transition must be considered carefully as the expansion is only quantitatively valid for small values of R .

IV. FURTHER INTERPRETATION OF THE PROFLIGACY FUNCTION

Consider a search company with K independent Brownian searchers each of fixed duration t_f , starting and resetting at the origin with fixed rate r in one dimension. For the moment, there is no target to search for. For each walker, there is a cost C_{traj} associated with its trajectory. The cost per walker $\sum_{\text{traj}} C_{\text{traj}}/K$ converges, for large K , to the mean cost $\langle C(r) \rangle$ associated with a trajectory of fixed duration t_f (irrespective of the target). The mean cost $\langle C(r) \rangle$ is an increasing function of r . Suppose that the total cost (or equivalently the mean $\langle C(r) \rangle$) is constrained to have a fixed value, say, C_0 (the fixed budget of the search company). Then, from $\langle C(r) \rangle = C_0$, one obtains a unique value of r , say, r_1 . This is the ‘predetermined’ search parameter estimated by the company, irrespective of where the target may lie.

Now, imagine putting a target at a distance m from the origin and the task of a searcher is to find the target in the least possible time, i.e., to maximize the success probability $P_s(r)$. However, the value r_2 , that maximizes $P_s(r)$ only, is typically not the same as r_1 (fixed by the budget). So, one needs to find a compromise. If we insist on a ‘fixed’ budget C_0 , then we have no choice but to select the predetermined value r_1 . One can optimize a bit better by choosing r to be different from the set value r_1 , i.e., by relaxing the hard cost constraint by a soft one. But this comes at a price. Allowing a bit more flexibility in the budget by exceeding C_0 incurs a penalty, parametrized by a temperature like factor $\lambda > 0$, as an additional weight factor $\exp \left[-\frac{1}{\lambda} (\langle C(r) \rangle - C_0) \right]$, for $\langle C(r) \rangle > C_0$. When $\lambda \rightarrow 0$, one recovers the hard constraint. Then our goal is to find the value of $r = r^*$ that maximizes the product of $P_s(r)$ and this weight factor. This is equivalent to minimizing the profligacy defined by

$$\xi = \langle C(r) \rangle - \lambda P_s(r) \quad (\text{S48})$$

where we have ignored a global constant involving C_0 without any loss of generality. Let us remark here that while the success probability $P_s(r)$ depends on the target distance m , the ‘predetermined’ reset parameter r_1 and cost function $\langle C(r) \rangle$ are independent of the target distance m .